THE ASTROPHYSICAL JOURNAL, 447:L109–L112, 1995 July 10

EGRET DETECTION OF PULSED GAMMA RADIATION FROM PSR B1951+32

P. V. RAMANAMURTHY,[1,2] D. L. BERTSCH,[1] B. L. DINGUS,[1,3] J. A. ESPOSITO,[1,3] J. M. FIERRO,[4] C. E. FICHTEL,[1] S. D. HUNTER,[1] G. KANBACH,[5] D. A. KNIFFEN,[6] Y. C. LIN,[4] A. G. LYNE,[7] J. R. MATTOX,[8] H. A. MAYER-HASSELWANDER,[5] M. MERCK,[5] P. F. MICHELSON,[4] C. VON MONTIGNY,[1,9] R. MUKHERJEE,[1,3] P. L. NOLAN,[4] AND D. J. THOMPSON[1]

Received 1995 March 13; accepted 1995 April 28

ABSTRACT

We detected a sixth high-energy gamma-ray pulsar, PSR B1951+32, pulsating in gamma rays at $E \geq 100$ MeV with the same 39.5 ms periodicity as in radio, using the data obtained during 1991 May to 1994 July by the Energetic Gamma Ray Experiment Telescope (EGRET) aboard the *Compton Gamma Ray Observatory*. Although seen only as a weak source amidst the high background of galactic disk emission, the pulsation in high-energy gamma rays is clearly seen. The pulsed radiation has a photon spectral index of -1.74 ± 0.11. There is no evidence as yet for unpulsed emission from the object. The pulsar appears to have an efficiency of $\sim$0.004 for converting its rotational energy loss into gamma rays at $E \geq 100$ MeV.

Subject headings: gamma rays: observations — pulsars: individual (PSR B1951+32)

1. INTRODUCTION

Discovered as a 39.5 ms radio pulsar in the radio synchrotron nebula CTB 80 by Kulkarni et al. (1988), PSR B1951+32 emits a single pulse at radio frequencies with a HWHM of approximately one-tenth of its period. From radio observations it is deduced (Taylor, Manchester, & Lyne 1993) that the object has a characteristic age of 1.1×10^5 yr, a surface magnetic field of 4.9×10^{11} G, and a rotation energy loss rate of 3.7×10^{36} ergs s^{-1} and is located at a distance of 1.5–3 kpc from Earth.

PSR B1951+32 has also been seen as a pulsating X-ray source by Ögelman & Buccheri (1987) in the *EXOSAT* data and more recently by Safi-Harb, Ögelman, & Finley (1995) in the *ROSAT* data. Li et al. (1987), using the *COS B* database and a period search technique, claimed to have seen high-energy gamma-ray (HEGR) pulsations from this object, but this was soon contradicted by D'Amico et al. (1987), who analyzed the same data. The effect claimed by Li et al. (1987) is well outside the reasonably expected range of periods. Later Bennett et al. (1990) analyzed the *COS B* data again near the expected range of periods and found an indication at a significance level of $\sim 10^{-3}$. Thompson et al. (1994) used the early Energetic Gamma Ray Experiment Telescope (EGRET) observations to set 99.9% confidence level upper limits of 1.4×10^{-7} and 3.6×10^{-7} photons cm^{-2} s^{-1} at $E \geq 100$ MeV for narrow (10%) and broad (50%) pulsed emissions, respectively, from this object; see also Brazier et al. (1994).

In this Letter, we present the details of observations (in § 2) and analysis and results (in § 3) establishing that the pulsar emits pulsed HEGR. We finally end with a discussion on the implications of our findings in § 4.

2. OBSERVATIONS

The EGRET detector is described by Kanbach (1989) and by Thompson et al. (1993). The latter reference gives many details of preflight and in-flight calibrations of the detector and data reduction procedures. For each event, energy, date, time in UTC (accurate to 100 μs), arrival direction, satellite location, and various other details are written into the summary database. EGRET has observed PSR B1951+32 in nine separate viewing periods at aspect angles (angle between the detector axis and the source direction) less than 20°. Details are given in Table 1.

3. ANALYSIS AND RESULTS

The arrival direction of a gamma ray is determined with an accuracy that is characterized by an energy-dependent point-spread function (PSF) given by (Thompson et al. 1993)

$$\theta_{0.67}(E) = 5.^\circ 85(100\ \mathrm{MeV}/E)^{0.534}, \tag{1}$$

where $\theta_{0.67}(E)$ is the half-angle of the cone around the true source direction containing 67% of the events at energy E. The source, PSR B1951+32, is located ($l = 68.^\circ 77$ and $b = 2.^\circ 82$) in a region of high Galactic background. This fact, combined with the rather large PSF given above, makes it difficult to detect a clear signal of pulsed gamma rays at low intensities, had we accepted all the events within the energy-dependent cone defined by equation (1). We have, therefore, made an energy-independent cut on the half-angle of the cone of acceptance centered on the pulsar direction. If the half-angle is too large, too many background events are admitted, submerging the signal. On the other hand, if the half-angle is too small, much of the signal also gets lost. As a compromise, and after trying five data selection cuts, we finally selected events from all the viewing periods at $E \geq 100$ MeV within a cone of a fixed half-angle of 1° with respect to the direction of the pulsar. A total of 344 gamma rays from all the viewing periods listed in

[1] Code 662, NASA Goddard Space Flight Center, Greenbelt, MD 20771.
[2] murthy@egret.gsfc.nasa.gov; NAS-NRC Senior Research Associate.
[3] USRA Research Associate.
[4] W. W. Hansen Experimental Physics Laboratory and Department of Physics, Stanford University, Stanford, CA 94305.
[5] Max-Planck-Institut für Extraterrestrische Physik, Giessenbachstrasse D-85748 Garching, Germany.
[6] Department of Physics, Hampden-Sydney College, Hampden-Sydney, VA 23943.
[7] Department of Physics, University of Manchester, Jodrell Bank, Macclesfield, SK11 9DL, UK.
[8] Compton Observatory Science Support Center, Computer Sciences Corporation, Greenbelt, MD 20770. Present address: Astronomy Department, University of Maryland, College Park, MD.
[9] NAS-NRC Research Associate.

TABLE 1

Details of Observations of PSR B1951+32

Viewing Period	Dates	Aspect Angle
0020	1991 May 30–Jun 8	4°5
0071	1991 Aug 8–15	11.3
2030	1992 Dec 1–22	9.3
2120	1993 Mar 9–23	17.3
3181	1994 Feb 1–8	3.2
3280	1994 May 24–31	4.8
3310	1994 Jun 7–10	4.8
3315	1994 Jun 14–18	4.8
3330	1994 Jul 5–12	4.8

Table 1 remained after this cut. Details of obtaining the light curves were discussed in the past EGRET publications (Nolan et al. 1993; Mayer-Hasselwander et al. 1994; Kanbach et al. 1994). The *contemporaneous* radio timing solutions we used in our analysis are given in Table 2, at three different epochs.

Figure 1 shows the light curve of gamma rays at $E \geq 100$ MeV from the pulsar, which exhibits two peaks at the phase values 0.16 and 0.60 with the convention that the radio peak (corrected to infinite frequency) occurs at phase 0.0. The second peak is broader than the first in the gamma-ray light curve. Neither of the peaks coincides with the radio peak position. There is no statistically compelling evidence for any intrapeak (bridge) emission. The χ^2 value for the distribution shown in Figure 1 is 133.3 for 49 degrees of freedom, which rules out the null hypothesis, i.e., there are no pulsations at a probability level of 10^{-9}. The bin-independent *H*-test (de Jaeger, Swanepoel, & Raubenheimer 1988) results in a value of 59.2, which implies once again that the null hypothesis is probable only at a level of less than 4×10^{-8}. The probabilities given here are for a single trial. Since we probed five different data selection cuts, these chance probabilities need to be multiplied by a factor of 5. Even then the null hypothesis is ruled out with a high statistical significance.

Assigning phase ranges 0.12–0.22 and 0.48–0.74 to the first and second peaks in Figure 1, respectively, and assuming that all gamma rays outside the peaks are due to background, the number of pulsed photons in each energy interval is calculated

TABLE 2

Radio Timing Parameters of PSR B1951+32

Parameter	Value
Right ascension (J2000)	$19^h52^m58^s.242$
Declination (J2000)	$+32°52'40''.96$
Frequency (Hz)	25.2969359550626
Frequency derivative......................	−3.74118E−12
Epoch (MJD)	48432.000000256[a]
Validity range (MJD).....................	48264–48601
Frequency (Hz)	25.2967530149361
Frequency derivative......................	−3.74216E−12
Epoch (MJD)	48998.000000235[a]
Validity range (MJD).....................	48898–49099
Frequency (Hz)	25.2966091636613
Frequency derivative......................	−3.74277E−12
Epoch (MJD)	49443.000000054[a]
Validity range (MJD).....................	49370–49516

[a] The fractional part of the epoch represents the arrival time of the first pulse after the integral number of modified Julian Dates of the epoch at the Earth geocenter, as in the format of the Princeton *GRO* database.

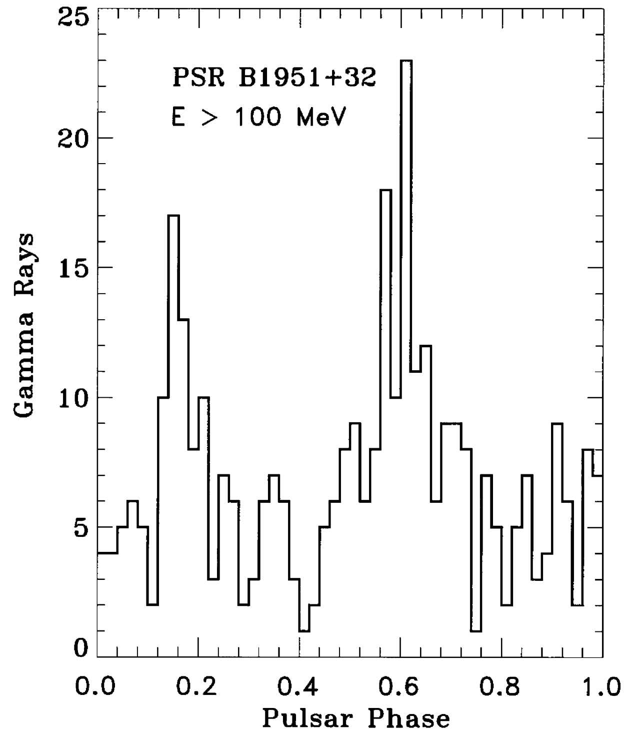

Fig. 1.—Light curve of the 344 gamma rays at $E > 100$ MeV within a fixed 1° radius circle around PSR B1951+32 from all the nine viewing periods listed in Table 1. The radio peak occurs at phase 0.0.

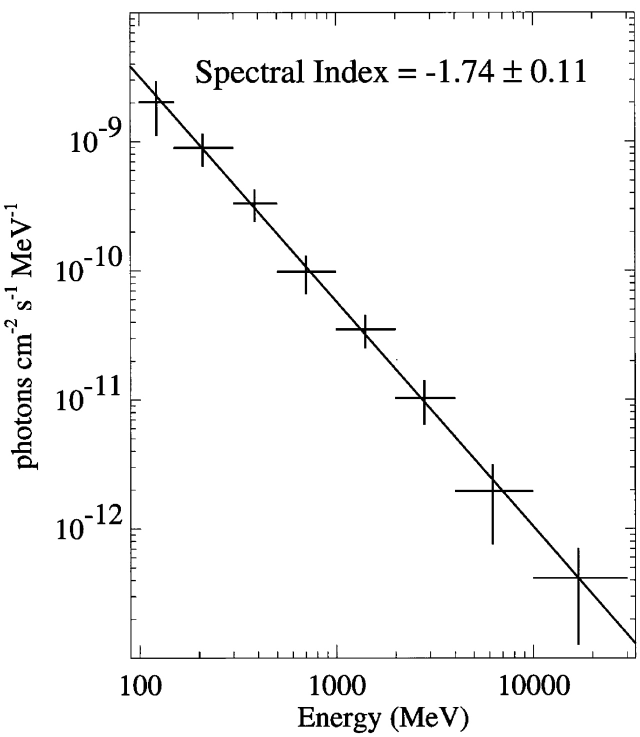

Fig. 2.—Phase-averaged differential energy spectrum of pulsed gamma rays at $E > 100$ MeV in the two peaks (see Fig. 1) after subtracting the background. The points are the data, and the straight line is the power-law fit given by eq. (2) with an exponent of −1.74.

TABLE 3

Observed Parameters of the Gamma-Ray Pulsars

Pulsar	l	b	P (s)	$\dot{P}$ (10^{-15} s s^{-1})	γ[a]	F_γ[b] (ergs cm^{-2} s^{-1})
Crab	184°6	−5°8	0.033	421	2.15	1.0E−9
Geminga	195.1	4.3	0.237	11.0	1.50	3.7E−9
Vela	263.6	−2.8	0.089	125	1.70	7.1E−9
B1055−52	286.0	6.6	0.197	5.83	1.18	4.2E−10
B1706−44	343.1	−2.7	0.102	93	1.72	8.3E−10
B1951+32	68.8	2.8	0.040	5.85	1.74	2.4E−10

[a] Exponent of the gamma-ray differential energy spectrum.
[b] F_γ is the observed gamma-ray energy flux.

after subtracting the background. A source power-law spectrum folded through the instrument response functions (Thompson et al. 1993) is then fitted to the resulting distribution of counts using a least-squares method. Figure 2 shows the resulting phase-averaged differential energy spectrum of the pulsed photons in the energy range 100 MeV–30 GeV. It is well represented by the power law given by

$$dN_\gamma/dE = (3.8 \pm 0.5) \times 10^{-11} \times (E/712\ \mathrm{MeV})^{-1.74\pm0.11}\ \mathrm{photons\ cm^{-2}\ s^{-1}\ MeV^{-1}}, \quad (2)$$

with E expressed in MeV. The exponent, -1.74 ± 0.11, indicates that the spectrum is slightly harder than that of the background diffuse radiation. The limited number of gamma rays does not let us determine the phase-resolved spectra. Using the likelihood analysis (Mattox et al. 1995), we estimate the total (pulsed + unpulsed) fluxes from the source as 6.0 ± 1.6 and 1.4 ± 0.6 in units of 10^{-8} photons cm^{-2} s^{-1} at energies greater than 300 and 1000 MeV, respectively. There is no evidence for emission below 300 MeV in the likelihood analysis, owing to the large Galactic background. Also, we find, using the cross-correlation technique (Hermsen 1980; Özel & Mayer-Hasselwander 1983), that the source stands out against the background much more clearly at higher energies. The integral of equation (3) results in an integral pulsed flux of $(1.6 \pm 0.2) \times 10^{-7}$ photons cm^{-2} s^{-1} at $E \geq 100$ MeV. This flux value is consistent within errors with the upper limits set by Thompson et al. (1994) and Brazier et al. (1994) using the early EGRET observations. Increased exposure to the pulsar is the main reason for the detection of pulsed signal in the present work. Assuming that gamma rays are emitted by the object as a beam of 1 sr in solid angle, the luminosity of the source in high-energy gamma rays is calculated to be $\sim 1.4 \times 10^{34}$ ergs s^{-1}, leading to an efficiency factor, $\eta \sim 0.004$, in converting the rotational energy loss of the pulsar into gamma rays.

4. DISCUSSION

Theoretical models to explain HEGR production by isolated pulsars fall into two general categories: polar cap models and outer gap models. Both types of models assume that HEGR are produced by a rotating magnetized neutron star with its magnetic axis making an angle with respect to its rotational axis. Briefly stated, in the polar cap models (see Harding & Daugherty 1993 and references therein), charged particles are accelerated in the electric fields developed near the polar caps of neutron stars and HEGR are produced by synchrotron emission and curvature radiation by the charged particles. In the outer gap models (see Cheng, Ho, & Ruderman 1986a, b; Ho 1993; Chiang & Romani 1993 and references therein), the particle acceleration takes place in the outer gaps much farther away from the magnetic poles, with HEGR emission taking place either by synchrotron radiation or inverse Compton scattering by the accelerated $e^\pm$ beams.

In the past Fierro et al. (1993) and Thompson et al. (1994) summarized the gamma-ray emission properties of the previously known five high-energy gamma-ray pulsars: Crab, Vela, Geminga, PSR B1706−44, and PSR B1055−52. Adding the results from the present work, we present the information on the observed and inferred parameters in Tables 3 and 4, respectively, for all six HEGR pulsars.

In comparison with the other gamma-ray pulsars, PSR B1951+32 has the lowest inferred surface magnetic field (4.9×10^{11} G), is the most (or among the most) distant, has the second smallest $\dot{P}$ value (5.85×10^{-15} s s^{-1}), is of median age (1.1×10^5 yr), and has the smallest observed gamma-ray flux. When the isolated spin-powered radio pulsars and Geminga are ranked according to the parameter $\dot{E}/d^2$ (where $\dot{E}$ is the rotation energy loss rate and d the distance), PSR 1951+32 ranks fifth, while the other HEGR pulsars rank 1, 2, 3, 6, and 24. The six HEGR pulsars are more or less confined to the Galactic disk, not unexpectedly like the distribution of all the

TABLE 4

Inferred Parameters of the Gamma-Ray Pulsars

Pulsar	Distance (kpc)	Age (yr)	B (G)	$\dot{E}$ (ergs s^{-1})	L_γ[a] (ergs s^{-1})	Efficiency[b] η
Crab	2.0	1.3E+3	3.8E+12	4.5E+38	3.9E+34	0.00009
Geminga	0.25	3.4E+5	1.6E+12	3.3E+34	2.2E+33	0.068
Vela	0.50	1.1E+4	3.4E+12	7.0E+36	1.7E+34	0.0024
B1055−52	1.5	5.3E+5	1.1E+12	3.0E+34	9.3E+33	0.31
B1706−44	1.8	1.7E+4	3.1E+12	3.4E+36	2.6E+34	0.0077
B1951 + 32	2.5	1.1E+5	4.9E+11	3.7E+36	1.4E+34	0.004

[a] L_γ is the gamma-ray luminosity.
[b] Proportional to the beaming factor.

radio pulsars. The phase separation between the two HEGR peaks is 0.44 in PSR B1951+32, which is in between those of the Crab and Vela pulsars (0.41) and that of Geminga (0.50). The HEGR peak positions do not coincide in phase with radio peaks, as in the case of Vela, PSR B1055−52 and PSR B1706−44 and unlike the Crab.

Safi-Harb et al. (1995) find that the pulsed X-ray peak from the present object approximately coincides in phase with the radio peak, unlike the positions of the HEGR peaks found here. The X-ray luminosity of the pulsar in the 0.1–2.4 keV band of *ROSAT* is $\sim 2.3 \times 10^{33}$ ergs s^{-1}, which is a factor of ~6 lower than the HEGR luminosity. Safi-Harb et al. (1995) conclude that the observed X-ray luminosity from the pulsar can be accounted for by the magnetospheric luminosity predicted by the model of Ögelman (1994).

In the polar cap model of Daugherty & Harding (1982), the quantity $\eta \dot{P}^{-1.3}$ is expected to be proportional to $\tau^{1.8}$ (Harding 1981), and Thompson et al. (1994) have shown that the five previously known HEGR pulsars are consistent with their prediction. Our present result on PSR B1951+32, too, is consistent with the prediction within the errors. Dermer & Sturner (1994) made predictions, based on their polar cap model, on the conversion efficiency, η, of rotation energy loss into gamma rays. Their prediction for PSR B1951+32 appears an order of magnitude lower than the one given in Table 4. In a revised outer gap model, Chen & Ruderman (1993) have indicated two allowed regions for HEGR pulsars in the dipole surface field–pulsar period parameter space. The present pulsar falls in the Vela-like region, above the death line, and is therefore consistent with the outer gap model too. While the observed flux of HEGR from PSR B1951+32 is in agreement with the prediction of Cheng & Ding (1994) based on a simplified outer gap model, it is much less than the prediction of Yadigaroglu & Romani (1995).

It is obvious that there are severe selection biases in detecting new HEGR pulsars, the most important factors being the flux, the relative geometry of radio and HEGR beams, and the background. The radio-quiet feature of Geminga is sometimes explained as a beaming effect (see, for example, Helfand 1994) with the Earth intercepting the HEGR beam but not the radio beam. Attention may be drawn here to the fact that four out of the top five isolated spin-powered radio pulsars ranked according to $\dot{E}/d^2$ are seen by us as gamma-ray pulsars, and even the fifth one, PSR B1509−58, was seen as a gamma-ray pulsar at $E < 2$ MeV by the other three detectors on the *Compton Gamma Ray Observatory*, though not by EGRET at $E > 50$ MeV. This remarkable success rate suggests that in most cases the radio and HEGR beams either are well aligned or are very broad, providing a good overlap between the two beams, despite the details of phase positions of the peaks. One has to consider the possible existence of more HEGR pulsars with similar, or somewhat weaker, fluxes and also the Geminga type, with undetected radio pulsations. The question of their contribution to the HEGR background (see, for example, Bailes & Kniffen 1992 and Hartmann & Brown 1994) may be reexamined with the additional information provided by the present pulsar.

The EGRET team gratefully acknowledges support from the following: Bundesministerium für Forschung und Technologie, grant 50 QV 9095 (MPE); NASA grant NAG5-1742 (HSC) and NASA grant NAG5-1605 (SU).

REFERENCES

Bailes, M., & Kniffen, D. A. 1992, ApJ, 391, 659
Bennett, K., et al. 1990, Proc. 21st Int. Cosmic Ray Conf. (Adelaide), 1, 181
Brazier, K. T. S., et al. 1994, MNRAS, 268, 517
Chen, K., & Ruderman, M. 1993, ApJ, 402, 264
Cheng, K. S., & Ding, W. K. Y. 1994, ApJ 431, 724
Cheng, K. S., Ho, C., & Ruderman, M. 1986a, ApJ, 300, 500
———. 1986b, ApJ, 300, 522
Chiang, J., & Romani, R. W. 1993, in Isolated Pulsars, ed. K. A. Van Riper, R. Epstein, & C. Ho (Cambridge: Cambridge Univ. Press), 287
D'Amico, N., et al. 1987, IAU Circ. 4507
Daugherty, J. K., & Harding, A. K. 1982, ApJ, 252, 337
de Jaeger, O. C., Swanepoel, J. W. H., & Raubenheimer, B. C. 1988, A&A, 221, 180
Dermer, C. D., & Sturner, S. J. 1994, ApJ, 420, L75
Fierro, J. M., et al. 1993, ApJ, 413, L27
Harding, A. K. 1981, ApJ, 245, 267
Harding, A. K., & Daugherty, J. K. 1993, in Isolated Pulsars, ed. K. A. Van Riper, R. Epstein, & C. Ho (Cambridge: Cambridge Univ. Press), 279
Hartmann, D. H., & Brown, L. E. 1994, in AIP Conf. Proc. 304, The Second Compton Symposium, ed. C. E. Fichtel, N. Gehrels, & J. P. Norris (New York: AIP), 101
Helfand, D. J. 1994, MNRAS, 267, 490
Hermsen, W. 1980, Ph.D. thesis, Univ. Leiden
Ho, C. 1993, in Isolated Pulsars, ed. K. A. Van Riper, R. Epstein, & C. Ho (Cambridge: Cambridge Univ. Press), 271
Kanbach, G. 1989, in Proc. *Gamma Ray Observatory* Science Workshop, ed. W. N. Johnson (Greenbelt: NASA Goddard Space Flight Center), 2-1
Kanbach, G., et al. 1994, A&A, 289, 855
Kulkarni, S. R., et al. 1988, Nature, 331, 50
Li, J. D., et al. 1987, IAU Circ. 4492
Mattox, J. R., et al. 1995, ApJ, submitted
Mayer-Hasselwander, H. A., et al. 1994, ApJ, 421, 276
Nolan, P. L., et al. 1993, ApJ, 409, 697
Ögelman, H. 1994, in Proc. NATO ASI on the Lives of Neutron Stars, ed. A. Alpar, Ü. Kiziloğlu, & J. van Paradijs (Dordrecht: Kluwer), 101
Ögelman, H., & Buccheri, R. 1987, A&A, 186, L17
Özel, M. E., & Mayer-Hasselwander, H. A. 1983, A&A, 125, 130
Safi-Harb, S., Ögelman, H., & Finley, J. P. 1995, ApJ, 439, 722
Taylor, J. H., Manchester, R. N., & Lyne, A. G. 1993, ApJS, 88, 529
Thompson, D. J., et al. 1993, ApJS, 86, 629
———. 1994, ApJ, 436, 229
Yadigaroglu, I.-A., & Romani, R. W. 1995, ApJ, in press